



Contents lists available at SciVerse ScienceDirect

Microvascular Research

journal homepage: www.elsevier.com/locate/ymvre

A natural antiviral and immunomodulatory compound with antiangiogenic properties

Carlos A. Bueno^a, María G. Lombardi^b, María E. Sales^b, Laura E. Alché^{a,*}

^a Laboratorio de Virología, Departamento de Química Biológica, Facultad de Ciencias Exactas y Naturales, Universidad de Buenos Aires, Pabellón II, Piso 4°, Ciudad Universitaria, C-1428GBA, Buenos Aires, Argentina

^b CEFYBO-CONICET, Segunda Cátedra de Farmacología, Facultad de Medicina, Universidad de Buenos Aires, Paraguay 2155 Piso 16°, CP 1121ABG, Buenos Aires, Argentina

ARTICLE INFO

Article history:

Accepted 13 September 2012

Available online xxxx

ABSTRACT

Meliacine (MA), an antiviral principle present in partially purified leaf extracts of *Melia azedarach* L., reduces viral load and abolishes the inflammatory reaction and neovascularization during the development of herpetic stromal keratitis in mice. 1-cinnamoyl-3,11-dihydroxymeliacarpin (CDM), obtained from MA, displays anti-herpetic and immunomodulatory activities *in vitro*. We investigated whether CDM interferes with the angiogenic process. CDM impeded VEGF transcription in LPS-stimulated and HSV-1-infected cells. It proved to have neither cytotoxic nor antiproliferative effect in HUVEC and to restrain HUVEC migration and formation of capillary-like tubes. Moreover, MA inhibits LMM3 tumor-induced neovascularization *in vivo*.

We postulate that the antiangiogenic activity of CDM displayed *in vitro* as a consequence of their immunomodulatory properties is responsible for the antiangiogenic activity of MA *in vivo*, which would be associated with the lack of neovascularization in murine HSV-1-induced ocular disease.

© 2012 Elsevier Inc. All rights reserved.

Introduction

Ocular Herpes simplex virus type 1 (HSV-1) infection may result in a chronic immunoinflammatory lesion in the corneal stroma termed herpetic stromal keratitis (HSK). The pathogenesis of HSK involves the production of proinflammatory cytokines and neovascularization of the normally avascular cornea (Biswas and Rouse, 2005; M. Zheng et al., 2001). Angiogenesis represents a major step in HSK pathogenesis, because neovessels permit the escape of cells and inflammatory molecules into stromal tissues, events that impair vision (Biswas and Rouse, 2005; M.E. Zheng et al., 2001). Preventing or limiting neovascularization is an effective strategy to control the severity of HSK (Carrasco, 2008; M.E. Zheng et al., 2001). The vascular endothelial growth factor (VEGF) is the main angiogenic molecule involved in the development of HSK. VEGF secretion is elicited in both, corneal epithelial cells and infiltrating macrophages, by IL-6 released from HSV-1-infected corneal epithelial cells (Biswas et al., 2006; M.E. Zheng et al., 2001). Besides, TNF- α counteracts the effect of VEGF on endothelial cells (EC), resulting in a blockade of corneal neovascularization *in vivo* (Fujita et al., 2007).

Topical corticosteroids and antivirals are the current therapy for HSK. Corticosteroids are known to combat the immunopathological component and antivirals prevent further viral replication. Although topical steroids shorten the course and prevent HSK progression, an

increase in recurrence and severity of disease in treated patients was reported, together with adverse effects, such as increased intraocular pressure, glaucoma and cataracts (Knickelbein et al., 2009). In addition, a recent study shows a high prevalence of HSV mutants resistant to acyclovir in comparison to that observed in immunocompetent individuals affected by other HSV-1 related diseases (Duan et al., 2008).

We have reported that meliacine (MA), an antiviral principle present in partially purified leaf extracts of *Melia azedarach* L., exerts a therapeutic effect on the development of HSK in mice by reducing viral load as well as by abolishing the ocular inflammatory reaction and neovascularization (Pifarré et al., 2002). Bioassay guided purification of MA led to the isolation of the limonoid 1-cinnamoyl-3,11-dihydroxymeliacarpin (CDM) that hinders HSV-1 multiplication (Alché et al., 2003; Barquero et al., 2006; Bueno et al., 2009). We found that CDM delays the transport of viral glycoproteins that would account for the strong inhibition on viral multiplication (Barquero et al., 2004; Bueno et al., 2010). CDM also decreases IL-6 production in HSV-1-infected corneal cells, enhances TNF- α and reduces IL-6 secretion when macrophages are either infected with HSV-1 or stimulated with LPS (Bueno et al., 2009).

Considering that IL-6 and TNF- α play an essential role in VEGF-induced corneal neovascularization process, we questioned whether CDM might interfere with the angiogenic process. Here we report that CDM has an anti-angiogenic effect and blocks proliferation, migration and tube formation *in vitro*. CDM decreases VEGF levels *via* reduction of cytokines that augment VEGF production in HSK. Moreover, MA restrains angiogenesis *in vivo* conditions.

* Corresponding author. Fax: +54 11 4576 3342.

E-mail address: lalche@qb.fcen.uba.ar (L.E. Alché).

Materials and methods

Cell culture, animals and viruses

Human Corneal-Limbal Epithelial (HCLE) cells were kindly provided by Dr. Argüeso (Harvard Medical School, Boston, USA) and grown in GIBCO Keratinocyte Serum Free Medium, supplemented with 25 µg/ml bovine pituitary extract, 0.2 ng/ml epidermal growth factor, and 0.4 mM CaCl₂, and maintained in low calcium DMEM/F12.

Murine macrophage cell line J774A.1 was kindly provided by Dr. Zabal (INTA-Castelar, Buenos Aires, Argentina) and grown in RPMI 1640 medium supplemented with 10% inactivated fetal bovine serum (FBS) and maintained in RPMI 1640 supplemented with 2% inactivated FBS.

Human Umbilical Vein Endothelial Cells (HUVEC) were cultured in EC growth M200 medium containing low serum growth supplement (Cascade Biologicals).

The LMM3 cell line was obtained from the spontaneous syngeneic mammary adenocarcinoma MM3 in the Angel H. Roffo Oncology Institute, (University of Buenos Aires, Argentina) (Urtreger et al., 1997) and cultured in DMEM/F12 medium with 2 mM L-glutamine, 80 µg/ml gentamycin, supplemented with 10% fetal calf serum (PAA laboratories GmbH).

Female BALB/c mice, three months old, were obtained from the School of Veterinary, University of Buenos Aires (Argentina). Animal care was provided in accordance with the procedure outlined in the Guide for Care and Use of Laboratory Animals (National Institute of Health, USA).

The HSV-1 KOS strain was propagated at low multiplicity.

Reagents

LPS from *E. coli* serotype O55: B5, TNF-α recombinant mouse, the goat polyclonal anti-TNF-α and anti-rabbit IgG conjugated with horseradish peroxidase were obtained from Sigma. Mouse monoclonal anti-IL-6 antibodies and recombinant human IL-6 were purchased from BD PharMingen. Rabbit polyclonal anti-VEGF-A antibodies were purchased from Santa Cruz Biotechnology, Inc. The VEGF-LUC reporter plasmid was kindly provided by Dr. Silberstein (School of Science, University of Buenos Aires, Argentina).

Preparation of MA and CDM

MA was partially purified from *Melia azedarach* L. according to the procedure described previously (Pifarré et al., 2002), and CDM was obtained from MA, as described by Alché et al. Due to the low mass availability of CDM, MA was used to perform *in vivo* experiments.

Transfection

Subconfluent cells grown on glass coverslips in 24-well plates were transiently transfected using Lipofectamine 2000 (Invitrogen) according to manufacturer's instructions. RSV-β-gal, coding for the bacterial β-galactosidase gene under the control of the viral RSV promoter, was used as second reporter control plasmid.

Cytotoxicity and antiproliferative assays

Cell viability was determined by using the tetrazolium salt MTT (3-(4,5-dimethylthiazol-2-yl)-2,5-diphenyltetrazolium bromide) (Sigma) (Denizot and Lang, 1986). For cell cytotoxicity, HUVEC were seeded at a concentration of 10⁴ cells/well in 96-well plates and grown at 37 °C for 24 h. Culture medium was replaced by medium containing CDM at various concentrations, in triplicate, and cells were incubated for 24 h. In the case of the antiproliferative assay, HUVEC were seeded at a concentration of 10⁴ cells/well in 96-well plates in the presence of different concentrations of CDM, and grown at 37 °C for 24 h. Afterwards, MTT reaction was performed and the absorbance

of each well was measured on an Eurogenetics MPR-A 4i microplate reader. Results were expressed as a percentage of absorbance of treated cell cultures with respect to untreated ones.

ELISA

TNF-α and IL-6 were quantified by commercial ELISA sets (BDOptEIAM, Becton Dickinson, USA) according to manufacturer instructions, in triplicate.

Chemotaxis assay

Cell migration was quantified using Transwell® Permeable Supports (Corning) (8 µm pore size), according to manufacturer's instructions. Briefly, the top chambers were seeded with HUVEC (4 × 10⁴ cell/well) in the presence of different concentrations of CDM, and the bottom chamber contained IL-6. HUVEC were allowed to migrate for 24 h at 37 °C. After incubation, cells on the top surface of the membrane (non-migrated) were scraped with a cotton swab. Cells on the bottom side (migrated cells) were stained with crystal violet. Images were obtained using an Olympus inverted microscope and migrating cells were quantified by manual counting. Percent inhibition of migrating cells was calculated with respect to untreated cells.

In vitro angiogenesis assay

Twenty four-well plates were coated with 100 µl Matrigel and incubated at 37 °C for 30 min. Then, HUVEC (8 × 10⁴ cells) were grown in Matrigel-coated plates for 24 h and treated simultaneously with different concentrations of CDM. In another set of experiments, HUVEC (8 × 10⁴ cells) grown in Matrigel-coated plates for 24 h, were treated, afterwards, with CDM during 24 h.

Tube formation was photographed using an Olympus inverted microscope (magnification: 400×). Tubular structures were quantified by manual counting in at least three fields, and the percentage of inhibition was calculated with respect to untreated cells.

Detection of VEGF-A by western blot (WB)

LMM3 (2 × 10⁶/well) was seeded in 6-well plates with 1 ml of DMEM/F12 and treated with MA (62.5 ng/µl), during 1 or 2 h. Then, supernatants were replaced by fresh medium and, after 24 h, were collected and stored at –80 °C. Cells were washed twice with PBS and lysed in 1 ml of modified RIPA buffer (Davel et al., 2004). After 1 h in ice, lysates were centrifuged at 10,000 rpm for 20 min at 4 °C. Supernatants were collected and protein concentration was determined by the method of Bradford.

Cell lysates and supernatants (80 µg protein/lane) were subjected to 10% SDS-PAGE minigel electrophoresis. Then, proteins were transferred to nitrocellulose membranes (BioRad) and blocked in 20 mM Tris-HCl buffer, 500 mM NaCl, and 0.05% Tween 20 (TBS-T) with 5% skimmed milk for 1 h at 20–25 °C. The nitrocellulose strips were incubated overnight with anti-VEGF-A diluted 1:100 in TBS-T. After several rinses with TBS-T, strips were incubated with the goat polyclonal anti-rabbit IgG (1:20,000) in TBS-T with 3% skimmed milk, at 37 °C during 1 h. Bands were detected by enhanced chemiluminescence substrate. Glycerinaldehyde 3-phosphate dehydrogenase (GAPDH) was used as loading control. Quantification of the bands was performed by densitometric analysis using Image J program (NIH), and expressed in optical density (O.D.) units relative to GAPDH.

Tumor induced angiogenesis

Tumor induced angiogenesis was quantified with an *in vivo* bioassay previously described (Davel et al., 2004). Briefly, LMM3 tumor cells were detached and washed twice with culture medium. Cell

concentration was adjusted to 2×10^6 cells/ml in DMEM/F12 medium, and were treated during 1 or 2 h with MA (62.5 ng/ μ l). After washing, cells ($2 \times 10^5/0.1$ ml) were inoculated intradermally in each flank of BALB/c mice. On day five animals were sacrificed and the inoculated sites were photographed under a dissecting microscope (Konus) ($6.4 \times$ magnification). Images were projected on a reticular screen to count the number of vessels per mm^2 of skin (Davel et al., 2004).

Statistical analysis

Statistical analysis of *in vitro* experiments was done by a Student's *t*-test, whereas ANOVA or Kruskal–Wallis tests were applied to the results obtained *in vivo*.

Results

Effect of CDM on VEGF transcription

Considering that CDM suppressed IL-6 production in J774A.1 and HCLE cells infected with HSV-1 and stimulated with LPS (Bueno et al., 2009), and that IL-6 can stimulate corneal cells and macrophages to secrete VEGF (Biswas et al., 2006; M.E. Zheng et al., 2001), we decided to investigate the effect of CDM on VEGF transcription.

HCLE and J774A.1 cells were transfected with a VEGF-LUC reporter plasmid and 24 h later, infected with HSV-1 (m.o.i. = 1). Then, CDM ($40 \mu\text{M}$) was added to cells during 8 h. HSV-1 infection augmented VEGF expression in both macrophages and corneal cells ($p < 0.01$). When VEGF-LUC-transfected and HSV-1-infected macrophages and corneal cells were supplied with CDM, VEGF expression was considerably reduced ($p < 0.05$). No significant differences between VEGF transcription from non-treated and CDM-treated cells were detected in uninfected cells (Figs. 1A and B).

On the other hand, LPS-stimulated macrophages revealed higher levels of VEGF in comparison to those observed in untreated cells

($p < 0.01$). In this case, CDM also proved to decrease the expression of VEGF ($p < 0.05$) (Fig. 1A).

Considering that HSV-1 and LPS stimulate cells to secrete IL-6, which in turn lead to VEGF production, we determined if CDM was able to affect VEGF expression in IL-6 stimulated cells.

HCLE and J774A.1 cells were transfected with a VEGF-LUC reporter plasmid during 24 h. Afterwards, cells were stimulated with 100 ng/ml of IL-6 and treated or not with CDM ($40 \mu\text{M}$) for 16 h. VEGF transcription was higher than that corresponding to untreated cells ($p < 0.01$). Conversely, CDM was not able to abrogate VEGF transcription induced by IL-6 (Figs. 1C and D).

Taken together, these results demonstrate that CDM impeded VEGF transcription in LPS-stimulated and HSV-1-infected cells, although it showed no effect when cells were stimulated with IL-6.

Effect of CDM on HUVEC viability, angiogenesis and chemotaxis

To explore antiangiogenic properties of CDM, we examined EC survival, capillary tube formation and migration.

To evaluate cytotoxic effect, HUVEC grown in 96-well plates were treated with CDM (5 – $100 \mu\text{M}$) and incubated at 37°C for 24 h. No cytotoxicity was found at all the concentrations tested, being the CC_{50} value higher than $100 \mu\text{M}$. When HUVEC were seeded together with CDM (5 – $100 \mu\text{M}$) and incubated at 37°C for 24 h, no antiproliferative effect was detected ($\text{IC}_{50} > 100 \mu\text{M}$) (data not shown).

The ability of CDM to prevent vessel assembly was analyzed by seeding HUVEC with CDM onto Matrigel layers for 24 h. Whereas HUVEC assembled into an extensive network of capillary-like structures within 24 h., CDM drastically inhibited ramifications in a dose-dependent manner, and undifferentiated round-shaped cells were observed (Fig. 2A).

In order to study if CDM affects the capillary-like network already established, HUVEC were grown in Matrigel-coated plates for 24 h. and then treated with CDM. At 24 h post-treatment (p.t.), we found

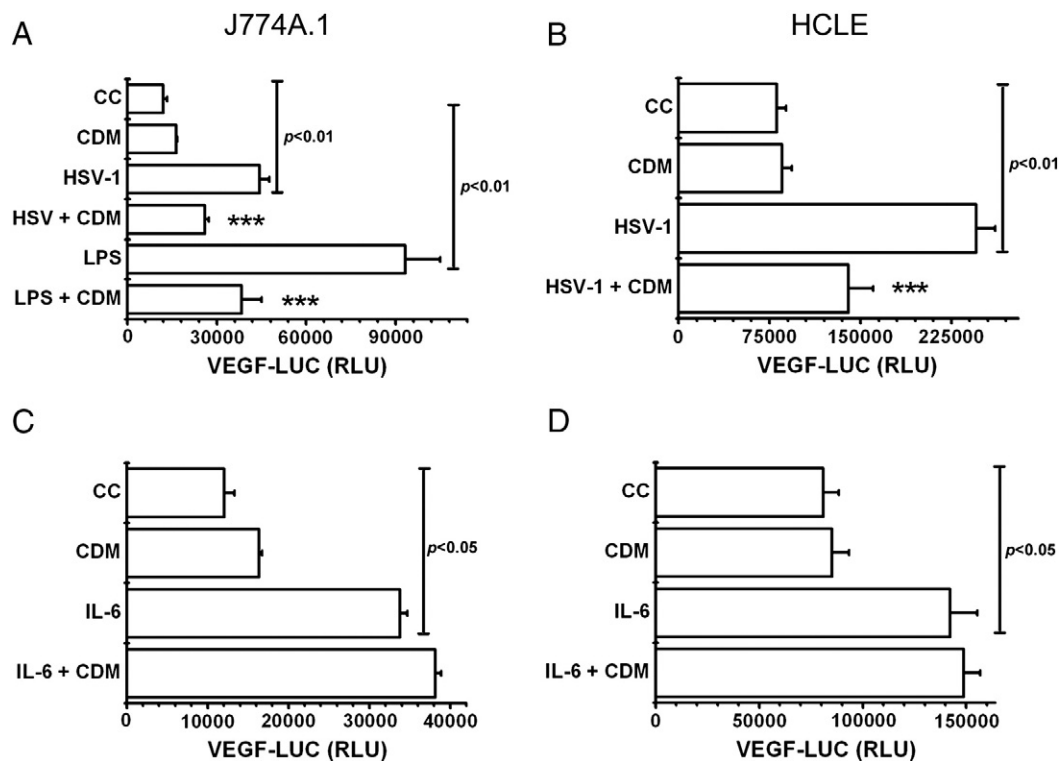


Fig. 1. Effect of CDM on VEGF transcription. J774A.1 and HCLE cells were transfected with 0.5 mg of VEGF-LUC reporter vector and 0.5 mg of β -galactosidase control plasmid. Twenty four hours post-transfection, J774A.1 and HCLE cells were treated with CDM ($40 \mu\text{M}$) and infected with HSV-1 (moi = 1) (A and B) and induced with IL-6 (100 ng/ml) for 16 h. (C and D). J774A.1 cells were also stimulated with LPS (100 ng/ml) for 8 h. (A). Luciferase activity was measured in cell extracts and each value was normalized to β -galactosidase activity in relative luciferase units (RLU). Data are expressed as the mean \pm S.D. of three separate experiments. (***) $p < 0.05$ compared to infected or stimulated cells.

that 80 μM of CDM disrupted the capillary-like network ($p < 0.05$) (Fig. 2B).

Hence, higher concentrations of CDM were required to disrupt the cord-like structures already established than those needed to impede tube formation (1.25 μM) ($p < 0.05$) (Figs. 2A and B).

In addition, CDM (40 μM) also reduced significantly IL-6-induced migration of HUVEC ($p < 0.05$) (Fig. 2C).

Effect of CDM on HUVEC cytokine production

To examine the influence of IL-6 and TNF- α on tubule formation, HUVEC grown in Matrigel-coated plates were cultured with or without these cytokines and specific antibodies against them, during 24 h. The addition of TNF- α (0.5 pg/ml) significantly suppressed vessel assembly (data not shown), while the addition of anti-TNF- α antibodies did not disrupt the cord-like structures (Fig. 3C). On the contrary, the supplement of IL-6 did not affect tubule formation (Fig. 3C), although it was

diminished when cells were treated with anti-IL-6 antibodies (data not shown).

Considering that TNF- α addition and IL-6 neutralization led to a disruption of tubule formation, we analyzed the effect of CDM on IL-6 and TNF- α secretion in HUVEC grown in Matrigel-coated plates for 24 h by ELISA.

HUVEC failed to produce TNF- α regardless that supernatants belonged to untreated or CDM-treated cells, whereas the levels of IL-6 were lesser in CDM-treated cell supernatants with respect to untreated ones (Figs. 3A and B).

To confirm that CDM modulates vessel assembly by inhibiting IL-6 secretion, we added IL-6 to CDM-treated cells. Therefore, HUVEC were seeded together with CDM (40 μM) and IL-6 (100 ng/ml) in Matrigel-coated plates during 24 h.

Unexpectedly, the number of cord-like structures detected in IL-6 + CDM-treated cells was lower than that obtained in untreated HUVEC ($p < 0.01$) (Fig. 3C). Similarly, the inhibition of tubule-like structures was

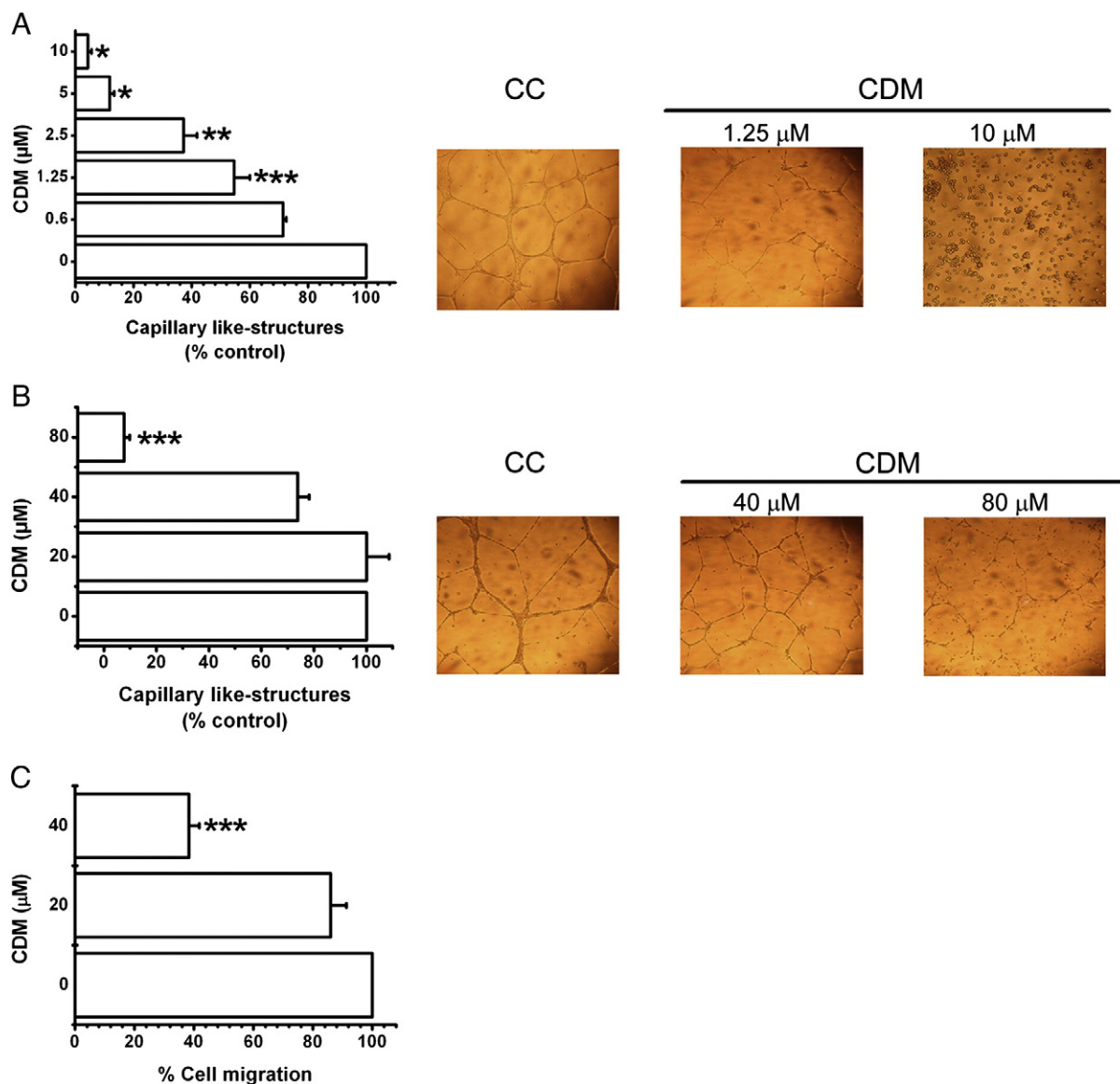


Fig. 2. Effect of CDM on capillary-like tube formation and chemotaxis. A) HUVEC were grown in Matrigel-coated plates and incubated with different concentrations of CDM. After 24 h, capillary-like structure formations were photographed and analyzed. Magnification: 400 \times . B) HUVEC were grown in Matrigel-coated plates for 24 h, and then treated with different concentrations of CDM. After 24 h, capillary-like structure formations were photographed and analyzed. Magnification: 400 \times . Data are expressed as mean percentage \pm SD of tube-like formation of three independent experiments. C) HUVEC migration was quantified in a Transwell membrane. The migrated cells were quantified by measuring the stained cells in at least five random areas per membrane. Data are expressed as mean percentage \pm SD of migrated cells of three independent experiments. (*) $p < 0.001$, (**) $p < 0.01$, (***) $p < 0.05$.

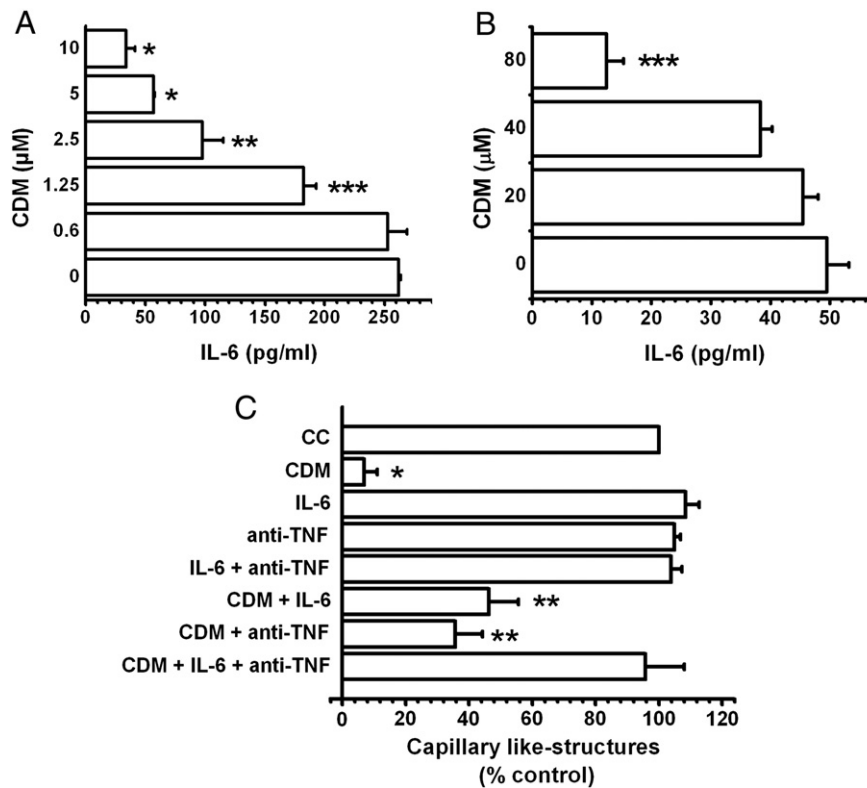


Fig. 3. Effect of CDM on cytokine production. A) HUVEC were grown in Matrigel-coated plates and incubated with different concentrations of CDM. After 24 h, IL-6 was determined by ELISA. B) HUVEC were grown in Matrigel-coated plates for 24 h and, then, treated with different concentrations of CDM. After 24 h, IL-6 was determined by ELISA. Data are expressed as the mean \pm S.D. of three separate experiments. C) HUVEC were grown in Matrigel-coated plates and incubated with CDM (40 μ M), IL-6 (100 ng/ml) and the anti-TNF- α antibody (1 μ g/ml). After 24 h, capillary-like structure formation was analyzed. Data are expressed as mean percentage \pm SD of tube-like formation from three independent experiments. (*) p <0.001, (**) p <0.01, (***) p <0.05.

not completely reverted when anti-TNF- α antibodies + CDM were added to HUVEC (p <0.01) (Fig. 3C). Nevertheless, no significant differences in the number of tubule-like structures in CDM + IL-6 + anti-TNF- α antibodies treated cells with respect to untreated HUVEC, were observed (Fig. 3C). Thus, the simultaneous addition of IL-6 and anti-TNF- α antibodies abolished the antiangiogenic activity of CDM *in vitro*.

In conclusion, CDM seemed to disrupt tubule formation in HUVEC as a consequence of the modulation in the production of both cytokines.

Effect of MA on tumor induced angiogenesis *in vivo*

First, we investigated the effect of MA on HUVEC capillary like-tube formation. Even concentrations as low as 50 ng/ μ l inhibited HUVEC tube formation (p <0.05), whereas 0.5 ng/ μ l did not significantly disrupt vessel assembly (data not shown). In addition, MA (62.5 ng/ml) was able to reduce the release of VEGF-A₁₆₅ to the supernatant of LMM3 cells, either after 1 or 2 h of treatment (p <0.01) (Fig. 4A), even though VEGF-A₁₆₅ was not significantly increased in the cellular lysate. Unexpectedly, VEGF-A₁₂₁ could not be detected in the supernatants belonging to either control or MA-treated cells; nevertheless, MA incremented the intracellular levels of VEGF-A₁₂₁ after 2 h. of treatment (p <0.001) (Fig. 4A). Moreover, when LMM3 cells were treated with the same concentration of MA by the same periods of time, and then were inoculated to syngeneic mice, it was effective in preventing tumor cell-induced neovascular response in the site of inoculation (p <0.001) (Fig. 4B).

Discussion

Neovascularization of the otherwise avascular cornea represents a pathological hallmark of ocular HSV-1 infection (Biswas and Rouse, 2005; M. Zheng et al., 2001; M.E. Zheng et al., 2001). Accordingly,

preventing, and ideally reversing neovascularization, is an important objective to retain optimal vision. In this sense, the treatment of HSK with antiangiogenic compounds has been proposed. Prior studies showed that counteracting VEGF significantly reduces HSV-1-induced angiogenesis (Carrasco, 2008; Cook and Figg, 2010; M.E. Zheng et al., 2001; Yeung et al., 2011). VEGF stimulates EC to migrate and form new vessels, events needed for the development of vasculature and proposed as targets for antiangiogenic compounds (Cook and Figg, 2010).

Many immune mediators like cytokines IL-1, IL-6, and TNF- α and various chemokines, such as IL-8, are also linked to angiogenesis (Albini et al., 2005; Cook and Figg, 2010; He et al., 2009; Lin et al., 2006). Several compounds derived from medicinal plants, such as epigallocatechin gallate (EGCG), resveratrol, wogonin and the terpenoids triptolide and celastrol, exhibit antiangiogenic properties as a consequence of the modulation of the immune response (Albini et al., 2005; He et al., 2009; Lin et al., 2006). We hypothesized that MA would block new vessel formation during HSK as a consequence of the immunomodulating effect of CDM observed *in vitro*.

In the present paper, we found that CDM inhibits VEGF transcription due to the reduction of IL-6 in corneal cells and macrophages infected with HSV-1 and stimulated with LPS (Fig. 1). It is known that TNF- α and IL-1 inhibit the signaling induced by IL-6 through different mechanisms in macrophages and epithelial cells, such as its receptor internalization and degradation (Radtke et al., 2010). However, we did not find any significant effect on the transcriptional activation of VEGF in CDM and IL-6 treated macrophages, even though CDM stimulates macrophages to secrete TNF- α (Fig. 1C) (Bueno et al., 2009). We cannot exclude that TNF- α secreted in CDM-treated cells can abrogate the signaling of IL-6 in HUVEC migration induced by IL-6 (Fig. 2C).

It is well-known that IL-6 exhibits a pro-angiogenic effect on HUVEC due to the stimulation of VEGF synthesis, which is produced by the activation of the transcription factor STAT3 (Ebrahim et al., 2006).

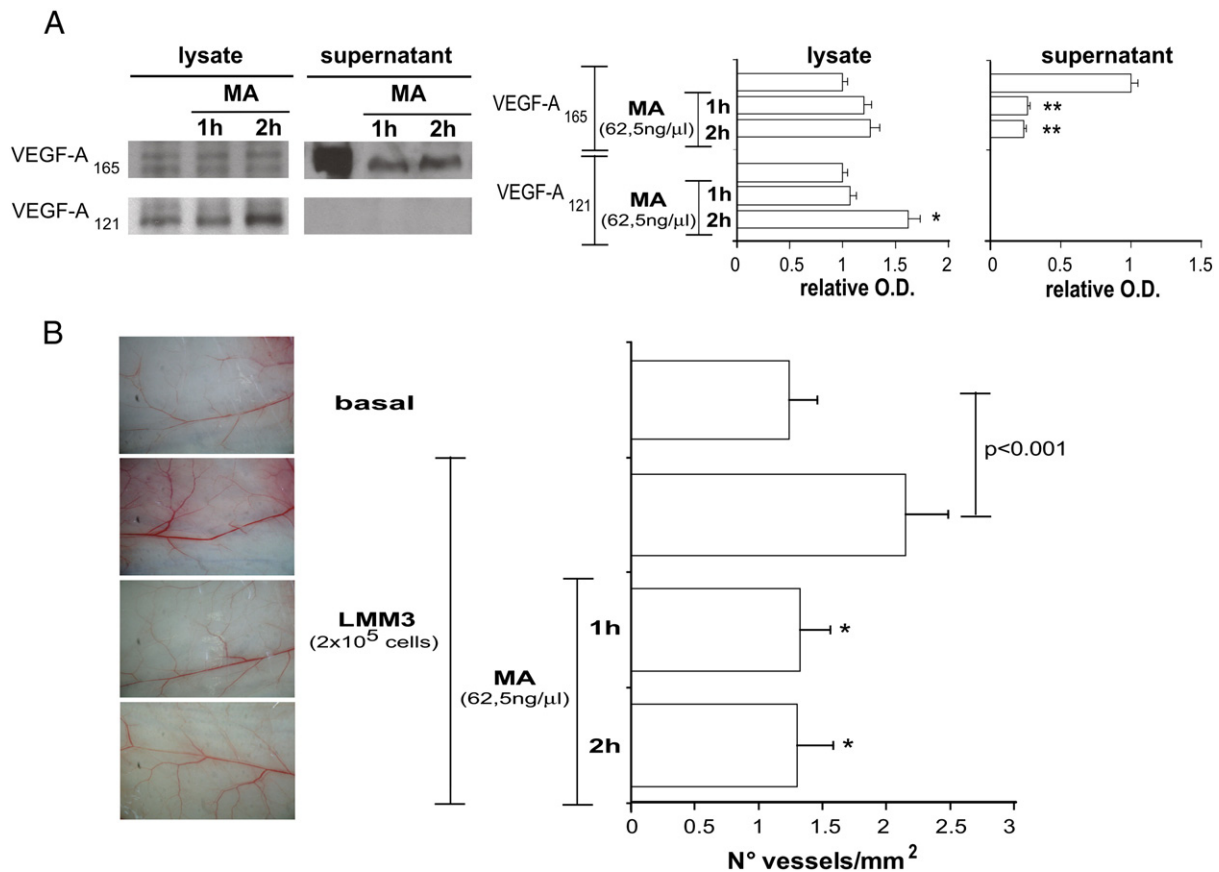


Fig. 4. Effect of MA on tumor induced angiogenesis. A) Western blot assay to detect vascular endothelial growth factor A (VEGF-A) in LMM3 cell lysates and supernatants (left panels). Tumor cells were treated with MA (62.5 ng/μl) during 1 or 2 h, by triplicate. Densitometric analysis of the bands was performed and optical density (O.D.) values are expressed with respect to glyceraldehyde 3-phosphate dehydrogenase for lysates, and with respect to control (untreated cells considered as 1) for supernatants (right panels). Values are mean ± SD of three independent experiments. ** $p < 0.01$; * $p < 0.001$. B) Photographs of the angiogenic site for each experimental group. Magnification: 6.4× (left panels). Quantification of the neovascular response expressed as number of vessels per square millimeter of skin (N° vessels/mm²) induced *in vivo* by LMM3 cells untreated or treated with MA during 1 or 2 h. Basal corresponds to vascular density of normal skin. Values are means ± S.D. of three experiments performed in triplicate. * $p < 0.001$ vs. control (untreated LMM3 cells) (right panel).

VEGF is the dominant factor in the induction of tubule formation by IL-6 (Hashizume et al., 2009).

Considering that HUVEC constitutes an experimental model of angiogenesis broadly employed to investigate the potential therapeutic use of new drugs in reducing pathological angiogenesis, we chose it to assay the antiangiogenic activity of CDM (De Luisi et al., 2009; Lin et al., 2006).

CDM inhibits the formation of capillary-like tubes in HUVEC as a consequence of the reduction of IL-6 and the enhancement of TNF-α (Fig. 3C). Given that higher concentrations of CDM are required to prevent the formation of new capillaries than those needed to disrupt previously assembled tubes (Figs. 2A and B), it could be useful as an antiangiogenic compound without side effects on mature vasculature.

MA hampered LMM3-induced neovascularization *in vivo*, probably by inhibiting VEGF-A₁₆₅ secretion (Fig. 4). Considering that CDM is able to affect the transcription and secretion of viral and cellular glycoproteins (Barquero et al., 2004, 2006; Bueno et al., 2009, 2010), we propose that MA would shift the balance in favor of the non-secreted VEGF-A₁₂₁ isoform at the expense of the secreted VEGF₁₆₅. Thus, the final effect observed would be the decrease of the total secretion of VEGF-A.

Conclusions

We postulate that the antiangiogenic properties of CDM displayed *in vitro* as a result of its immunomodulatory activity, are responsible for the antiangiogenic activity of MA *in vivo*. The availability of a compound as CDM, gathering together antiviral, immunomodulatory and antiangiogenic properties, will make it an excellent candidate

as a novel anti-HSV-1 agent, and, in extent, suitable for the treatment of an immunopathology in which the immune response and the angiogenesis are the main pathogenic factors.

Acknowledgments

The authors wish to thank Isabel Paz and Guillermo Assad Ferek for their technical assistance. This work was supported by grants from the CONICET (PIP 1007) and Universidad de Buenos Aires (UBA) (UBACyT X002 and UBACyT M064).

References

- Albini, A., Tosetti, F., Benelli, R., Noonan, D.M., 2005. Tumor inflammatory angiogenesis and its chemoprevention. *Cancer Res.* 65, 10637–10641.
- Alché, L.E., Assad Ferek, G., Meo, M., Coto, C., Maier, M., 2003. An antiviral meliicarpin from leaves of *Melia azedarach* L. *Z. Naturforsch. C* 58, 215–219.
- Barquero, A.A., Alché, L.E., Coto, C., 2004. Block of vesicular stomatitis virus endocytic and exocytic pathways by 1-cinnamoyl-3,11-dihydroxymeliicarpin, a tetranortriterpenoid of natural origin. *J. Gen. Virol.* 85, 483–493.
- Barquero, A.A., Michelini, F.M., Alché, L.E., 2006. 1-Cinnamoyl-3,11-dihydroxymeliicarpin is a natural bioactive compound with antiviral and nuclear factor-kappaB modulating properties. *Biochem. Biophys. Res. Commun.* 344, 955–962.
- Biswas, P.S., Rouse, B.T., 2005. Early events in HSV keratitis – setting the stage for a blinding disease. *Microbes Infect.* 7, 799–810.
- Biswas, P.S., Banerjee, K., Kinchington, P.R., Rouse, B.T., 2006. Involvement of IL-6 in the paracrine production of VEGF in ocular HSV-1 infection. *Exp. Eye Res.* 82, 46–54.
- Bueno, C.A., Barquero, A.A., Di Cónsoli, H., Maier, M.S., Alché, L.E., 2009. A natural tetranortriterpenoid with immunomodulating properties as a potential anti-HSV agent. *Virus Res.* 141, 47–54.
- Bueno, C.A., Alché, L.E., Barquero, A.A., 2010. 1-Cinnamoyl-3,11-dihydroxymeliicarpin delays glycoprotein transport restraining virus multiplication without cytotoxicity. *Biochem. Biophys. Res. Commun.* 393, 32–37.

- Carrasco, M.A., 2008. Subconjunctival bevacizumab for corneal neovascularization in herpetic stromal keratitis. *Cornea* 27, 743–745.
- Cook, K.M., Figg, W.D., 2010. Angiogenesis inhibitors: current strategies and future prospects. *CA Cancer J. Clin.* 60, 222–243.
- Davel, L.E., Rimmaudo, L., Español, A., De La Torre, E., Jasnis, M.A., Ribeiro, M.L., Gotoh, T., de Lustig, E.S., Sales, M.E., 2004. Different mechanisms lead to the angiogenic process induced by three adenocarcinoma cell lines. *Angiogenesis* 7, 45–51.
- De Luisi, A., Mangialardi, G., Ria, R., Acuto, G., Ribatti, D., Vacca, A., 2009. Anti-angiogenic activity of carebazine: a plausible mechanism affecting airway remodelling. *Eur. Respir. J.* 34, 958–966.
- Denizot, F., Lang, R., 1986. Rapid colorimetric assay for cell growth and survival. Modifications to the tetrazolium dye procedure giving improved sensitivity and reliability. *J. Immunol. Methods* 89, 271–277.
- Duan, R., de Vries, R.D., Osterhaus, A.D., Remeijer, L., Verjans, G.M., 2008. Acyclovir-resistant corneal HSV-1 isolates from patients with herpetic keratitis. *J. Infect. Dis.* 198, 659–663.
- Ebrahim, Q., Minamoto, A., Hoppe, G., Anand-Apte, B., Sears, J., 2006. Triamcinolone acetonide inhibits IL-6 and VEGF-induced angiogenesis downstream of the IL-6 and VEGF receptors. *Invest. Ophthalmol. Vis. Sci.* 47, 4935–4941.
- Fujita, S., Saika, S., Kao, W., Fujita, K., Miyamoto, T., Ikeda, K., Nakajima, Y., Ohnishi, Y., 2007. Endogenous TNF α suppression of neovascularization in corneal stroma in mice. *Invest. Ophthalmol. Vis. Sci.* 48, 3051–3055.
- Hashizume, M., Hayakawa, N., Suzuki, M., Mihara, M., 2009. IL-6/sIL-6R transsignalling, but not TNF- α induced angiogenesis in a HUVEC and synovial cell co-culture system. *Rheumatol. Int.* 29, 1449–1454.
- He, M.F., Liu, L., Ge, W., Shaw, P.C., Jiang, R., Wu, L.W., But, P.P., 2009. Antiangiogenic activity of Tripterygium wilfordii and its terpenoids. *J. Ethnopharmacol.* 121, 61–68.
- Knickelbein, J.E., Hendricks, R.L., Charukamnoetkanok, P., 2009. Management of herpes simplex virus stromal keratitis: an evidence-based review. *Surv. Ophthalmol.* 54, 226–234.
- Lin, C.M., Chang, H., Chen, Y.H., Li, S.Y., Wu, I.H., Chiu, J.H., 2006. Protective role of wogonin against lipopolysaccharide-induced angiogenesis via VEGFR-2, not VEGFR-1. *Int. Immunopharmacol.* 6, 1690–1698.
- Pifarré, M.P., Berra, A., Coto, C.E., Alché, L.E., 2002. Therapeutic action of meliacine, a plant-derived antiviral, on HSV-induced ocular disease in mice. *Exp. Eye Res.* 75, 327–334.
- Radtke, S., Wüller, S., Yang, X., Lippok, B.E., Mütze, B., Mais, C., de Leur, H.S., Bode, J.G., Gaestel, M., Heinrich, P.C., Behrmann, I., Schaper, F., Hermanns, H.M., 2010. Cross-regulation of cytokine signaling: pro-inflammatory cytokines restrict IL-6 signaling through receptor internalization and degradation. *J. Cell Sci.* 123, 947–959.
- Urtreger, A., Ladedá, V., Puricelli, L., Rivelli, A., Vidal, M., Delustig, E., Joffe, E., 1997. Modulation of fibronectin expression and proteolytic activity associated with the invasive and metastatic phenotype in two new murine mammary tumor cell lines. *Int. J. Oncol.* 11, 489–496.
- Yeung, S.N., Lichtinger, A., Kim, P., Amiran, M.D., Slomovic, A.R., 2011. Combined use of subconjunctival and intracorneal bevacizumab injection for corneal neovascularization. *Cornea* 30, 1110–1114.
- Zheng, M., Schwarz, M.A., Lee, S., Kumaraguru, U., Rouse, B.T., 2001a. Control of stromal keratitis by inhibition of neovascularization. *Am. J. Pathol.* 159, 1021–1029.
- Zheng, M.E., Deshpande, S., Lee, S., Ferrara, N., Rouse, B.T., 2001b. Contribution of vascular endothelial growth factor in the neovascularization process during the pathogenesis of herpetic stromal keratitis. *J. Virol.* 75, 9828–9835.